Chapter 13 – NUMERICAL SOLUTIONS FOR THE CAWAPI CONFIGURATION ON UNSTRUCTURED GRIDS AT LOCKHEED MARTIN, UNITED STATES

by

M. Bruce Davis, Christopher L. Reed and Patrick J. Yagle

13.1 SUMMARY

As part of the Cranked Wing Aerodynamics Project International (CAWAPI), computational fluid dynamics (CFD) simulations were performed on the F-16XL geometry at high-lift and transonic flight conditions. This was part of a larger effort by several institutions and companies to try to characterize the relevant flow physics and to compare the results to flight test data. The work summarized in this report used the Lockheed Martin Aeronautics Company proprietary CFD flow solver Falcon v4, which is a general purpose Navier-Stokes flow solver which uses hybrid unstructured computational meshes. The computational mesh used in these studies consisted of prismatic and hexahedral cells near the solid surfaces, tetrahedral cells in the far field, and pyramidal cells transitioning between hexahedral and tetrahedral cells. This mesh was obtained from the UT SimCenter and was generated using Gridgen for the inviscid mesh and proprietary software to generate the viscous prismatic layers. The results on a set of test cases selected by the CAWAPI task group shows good agreement with the flight test data and consistency with the other computational results for the high-lift cases, with the exception of the leading edge suction peak. The key flow features of these types of configurations, including the primary vortex originating on the inboard leading edge of the wings, the secondary vortex on the aft portion of the wing next to the primary vortex, and the vortices shed from the wingtip missile fins are all adequately resolved. The transonic flight test case, which has caused some difficulty because of the nonlinear nature of the flow physics, did not match flight test data as well. The reason for the discrepancies are unknown at the present time, but the consistency of these discrepancies across a range of different flow solvers and grids suggests that there is a difference between the configuration and flow conditions in the test and those simulated in the CFD. A brief description of the simulations performed is presented below, a description of the Falcon v4 CFD solver is presented, and a summary of the results is presented and explained.

13.2 INTRODUCTION

The Cranked Arrow Wing Aerodynamics Project International (CAWAPI) was a combined flight test, wind tunnel test, and computational program which used the F-16XL aircraft to characterize and document the flow physics on the wing upper surface for aircraft configurations representative of the F-16XL, with emphasis on high-lift and transonic flight conditions [13-1],[13-2]. The CAWAPI program was also to provide a test data suite which could be used to compare and improve computational fluid dynamics (CFD) simulations for these configurations. The CFD solutions could also be used as an additional source of flow data to augment the flight and wind tunnel data.

The F-16XL was designed jointly by General Dynamics Corporation-Fort Worth (now Lockheed Martin Aeronautics Company (LM Aero)) and NASA Langley Research Center, and built by General Dynamics. The aircraft is based on the F-16 with the fuselage lengthened and a cranked-arrow wing replacing the existing wing. The wing has a leading edge sweep of 70 degrees inboard and 50 degrees outboard of the crank, and is

blended to the fuselage with an S-curve. Air dams are installed at the centerline of the actuator pod just inboard of the crank. The flight test configuration of the F-16XL is shown in Figure 13-1.

Figure 13-1: Flight Test Configuration of the F-16XL.

A variety of flight test data was taken, including surface static pressures, boundary layer rake pressures, hot-film, and surface visualization including tufts, oil, and liquid-crystals. The data most relevant to the present work is the surface pressure data collected by both flush ports and belts at certain Butt Line (BL) and Fuselage Station (FS) lines. CFD data are compared to the flight test data mainly by comparing pressures at these BL and FS cuts.

The computational effort for this particular program has focused on a set of seven flight configurations. A complete description of the flight conditions with relevant engine parameters is given in [13-2]. A summary of these conditions is shown in Table 13-1. There are five conditions with no appreciable sideslip, and two cases which include significant sideslip. All of the flight test cases are at low speed (Mach number less than .5) and high angle of attack (greater than ten degrees), with the exception of the single transonic case (M = 0.97), for which the angle of attack is 4.37 degrees. The flow Reynolds number based on the mean aerodynamic chord varies from 32 million to 89 million for the transonic case. Due to the time limitation, LM Aero concentrated on three different flight conditions, all of which are at zero nominal sideslip. The solutions are all run with a half-symmetry model. The flight conditions simulated at LM Aero (shown in red in Table 13-1) are FC7, FC19, and FC70. FC7 and FC19 are high-lift cases and FC70 is a transonic case.

Table 13-1: The CAWAPI Program Examined Seven Different Flight Conditions

Flight Condition	Actual Mach	Actual α	Actual β	Actual Re
FC7	0.304	11.89	-0.133	44.4×10^6
FC19	0.360	11.85	0.612	46.8×10^6
FC46	0.527	10.4	0.684	46.9×10^6
FC70	0.97	4.37	0.310	88.77×10^6
FC25	0.242	19.84	0.725	32.22×10^6
FC50	0.434	13.56	5.31	39.41×10^6
FC51	0.441	12.89	-4.58	38.95×10^6

LM Aero has developed and maintains a proprietary CFD solver called Falcon, and the latest version (v4) has added unstructured grid capability. Supported cell types include hexahedral, tetrahedral, pyramid, and prismatic cells. Falcon is a general purpose flow solver, having been used for external aerodynamics, nozzle and duct flows, low speed aircraft environment flows, and transonic and supersonic flows.

LM Aero, which designed and built the F-16XL, contributed the original computational geometry for the program. The company then contributed to the program in an observation and consultation capacity only, providing such data as engine parameters and flap settings. As a separate effort, LM Aero conducted a grid challenge in which several different grid vendors were asked to generate and submit a computational mesh for the F-16XL geometry appropriate for a simulation at one of the high-lift flight conditions. The submitted grids were evaluated by the LM Aero staff and an attempt was made to run the simulation on different CFD solvers used at LM Aero, including Falcon v4. Late in the CAWAPI effort, the CAWAPI suite was selected as a validation case for Falcon v4, which was nearing production release at the time. The results submitted here are the direct outgrowth of that validation effort.

13.3 FALCON V4

Falcon is a finite-volume computational fluid dynamics (CFD) system that has been developed and maintained by the Lockheed Martin Aeronautics (LM Aero) Aerodynamics and CFD Branch. Development of the code was initiated in the late 1980's and starting in the early 1990's the code became and continues to be routinely used on a number of aircraft programs and development projects at LM Aero, as well as several other Lockheed Martin Corporation, partner and government sites. In 2002 an effort was initiated to rewrite the code in a more modern form and allow multiple element types (hybrid grids). The desire was to expand the code's capability to use various grid types while retaining the accuracy and unique features of previous versions of Falcon. The rewrite also provided an opportunity to improve the code's user interface and maintainability. The improved code was designated version 4 (v4).

Falcon v4 is actually a system of codes that make use of a modular architecture that incorporates some object-oriented programming concepts. The software is designed to be modular to allow quick development of required aerodynamic analysis capabilities. Falcon v4 uses hybrid unstructured grids that may include a variety of cell (element) shapes. The majority of the code is written in a modern-style Fortran 90 that makes heavy use of

derived data types and modules. In order to implement this style, the code development process uses templates and code generated automatically by programs written in the Python programming language. This approach provides a much easier technology insertion capability, allows the solver to be used as an engine in other applications, and allows applications specific capabilities to be developed. All components of the Falcon v4 CFD system are compiled from the same source code to ensure consistency and to reduce maintenance requirements. Considerable effort has been taken in the design of the code to optimize it for efficient operation on commodity cache-based processors, while maintaining the ability to run efficiently on vector architectures as well.

The user interface to the Falcon v4 system has been greatly simplified from previous versions of Falcon. The interface starts with the Falcon v4 pre-processor which can be run in an interactive, interview-style mode or can be run in a batch mode. Queries and/or inputs to the system are intuitive and all inputs are stored for reuse and archival purposes. The Falcon v4 system also makes use of a unique perfect gas conditions calculator which assists in setting up consistent flow field conditions.

The governing equations in the Falcon v4 solver are the Reynolds averaged, compressible Navier-Stokes equations. A steady-state solution to the governing equations is obtained by using an implicit time marching scheme with upwind differenced fluxes for the inviscid terms and central differenced fluxes for the viscous terms. Inviscid fluxes are computed using Roe's approximate Riemann solver [13-3]. The primitive variables (ρ, u, v, w and T) are extrapolated to the face for higher order accuracy. Viscous fluxes are computed from gradient estimates at the cell faces. The face gradients are calculated as the distance weighted average of the gradients at the centroids of the two cells on either side of the face. The component normal to the interface is then replaced with the local information. The Falcon code includes the two-equation k-kl turbulence model by Smith [13-4] (with an algebraic stress model option) for accurate turbulence calculations. For unsteady calculations, an LES model can be used. A wall-layer model (or wall function) is generally used to reduce the number of points required for accurate boundary layer calculations.

A highly implicit numerical solver has been implemented using incomplete lower-upper (ILU) factorization. The implicit Jacobians are stored such that they do not need to be calculated at each time-step. This variable update of the Jacobians significantly reduces CPU time. All of the boundary conditions are applied/computed implicitly. The code also includes the capability to accurately solve very low speed and mixed speed flows using low speed preconditioning [13-5]. Currently, the code can be run with any of several different gas models. These include constant gamma, variable gamma as a function of temperature for air, variable gamma for a typical jet engine exhaust, or a four species flow model.

Although the code uses non-dimensional values internally, inputs to the code and outputs from the code can be in either English or SI units. The code can perform accurate unsteady (time-accurate) analyses using subiterations. Falcon v4 is set-up to efficiently perform on a parallel computer using the standard message passing interface (MPI), with domain decomposition produced by the METIS algorithm [13-6]. For restart files, grids and boundary condition specifications, the code uses an enhanced, self describing, platform independent file system to facilitate working on a heterogeneous computer network. A number of features of Falcon v4 have been developed/implemented to significantly reduce workload and provide a process that is completely consistent with LM Aero engineering processes and tools. Other code features include a variety of boundary condition types and a number of LM proprietary models that have been required for advanced development activities.

User oriented features include the capability to pick the flow output parameters from a menu of choices and then output that data to a file or files specified by the user. In this way an engineer can monitor the convergence of lift, drag, mass flow, thrust, pressure recovery, or any number of other integrated quantities.

13.4 F-16XL GEOMETRY AND COMPUTATIONAL GRID

The F-16XL was designed at LM Aero, and hence the geometry files were available in electronic format within the company. This geometry did require some preparation, however. All modifications to the geometry were made using Lockheed Martin's proprietary computer-aided design software. Existing gaps in the geometry were corrected to provide as water-tight a geometry definition as possible for CFD analysis. In order to simplify mesh generation, several aircraft features were simplified. The gap between the tip missile and the missile rail was filled. The gaps between the nozzle and the speed brakes on either side of the nozzle were filled. Lastly, the gap between the nozzle and the bottom of the vertical tail was filled. For all of the analyses, the aircraft control surfaces remain fixed and undeflected. All gaps related to the control surfaces are filled and were not modeled. All other aerodynamic features of the aircraft were modeled. The surface mesh on the top and bottom surfaces is shown in Figure 13-2. This shows the grid clustering near the leading edge, along the air dam and around the actuator pod, at the wing-fuselage junction, and a high grid density outboard of the crank and on the tip missile. Figure 13-3 shows the surface grid on the symmetry plane, with the obvious clustering near the aircraft surface transitioning to a much coarser mesh in the far field.

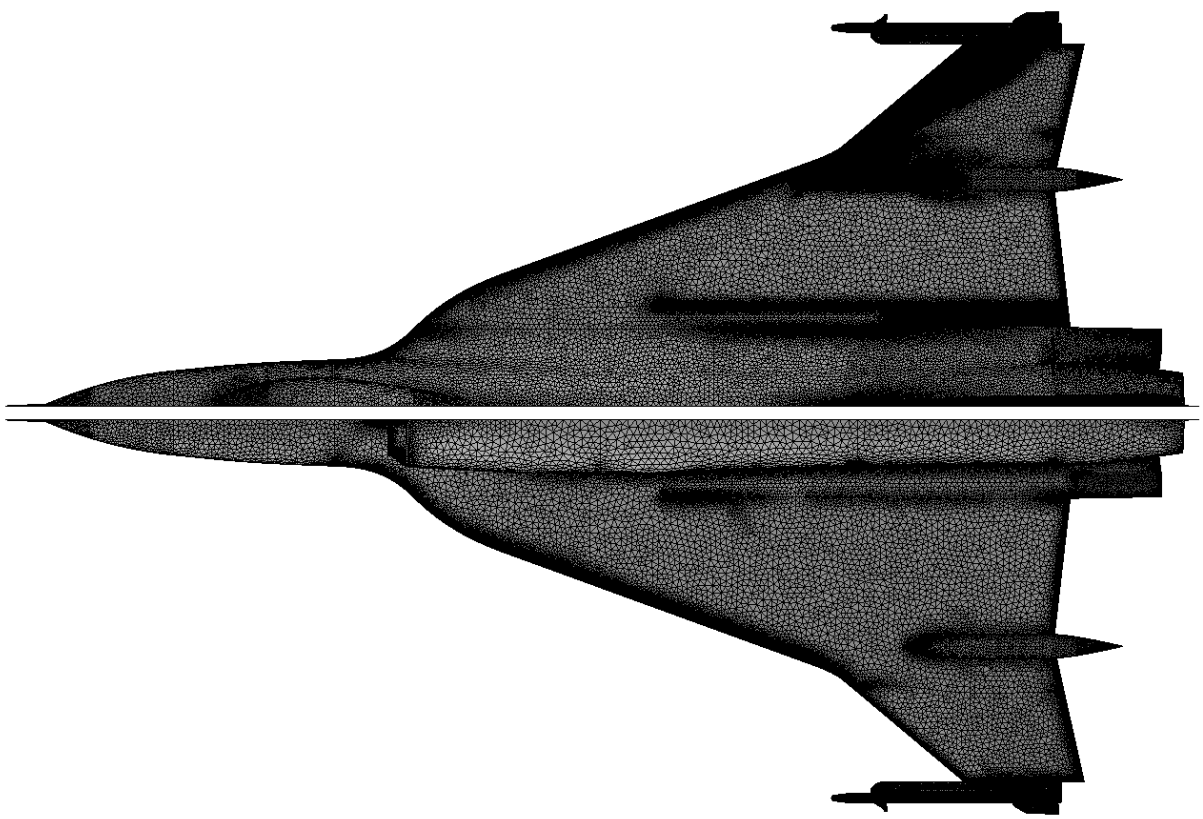

Figure 13-2: Top and Bottom Surface Grid of F-16XL Shows Clustering at Key Locations.

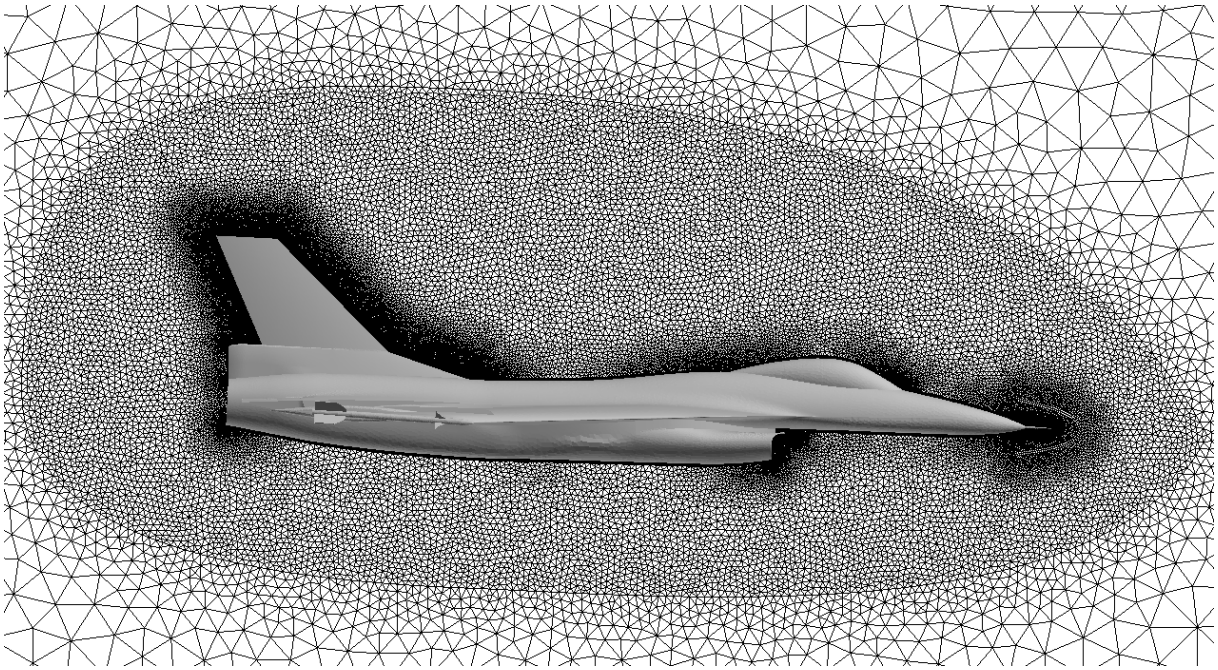

Figure 13-3: Surface Grid on the Symmetry Plane is Clustered Near the Aircraft.

The computational mesh for these analyses was provided to LM Aero by Dr. Steve Karman at the University of Tennessee SimCenter [13-7]. The grid was generated using two different mesh generation programs. The inviscid mesh was generated using the commercially available Gridgen software package. The surface mesh consists of triangular elements with proper resolution of the various features of the aircraft. Structured quadrilateral elements were used to mesh the leading and trailing edges of the wing. These quadrilaterals were then split into triangles in order to obtain anisotropic triangular mesh elements. Additionally, baffle surfaces were used to control mesh spacing in key areas of the inviscid volume mesh. A mesh generation program developed at the UT SimCenter was used to add viscous layers to the inviscid mesh already obtained [13-8]. The program adds viscous layers by pushing the existing mesh away from the aircraft surface, and then filling in with triangular prisms (see [13-8] for details of the algorithm). The number of prism layers varies locally based on the distance the inviscid mesh has been pushed away from the surface. A wall-normal spacing appropriate to the application of wall-function boundary conditions was chosen. The final mesh contains 32,415,471 tetrahedra, 9,612,208 triangular prisms, 212,408 hexahedra, and 188,175 pyramid mesh elements. A crinkle cut of the grid through the missile fins is shown in Figure 13-4. Note the thin prismatic cells near the surface transitioning to the tetrahedral further out. The large size of this problem necessitated simulation in a parallel environment. The final mesh was partitioned into 64 subdomains using the METIS partitioning software [13-6]. This decomposition is shown colored by process number in Figure 13-5. All results were generated on 64 processors.

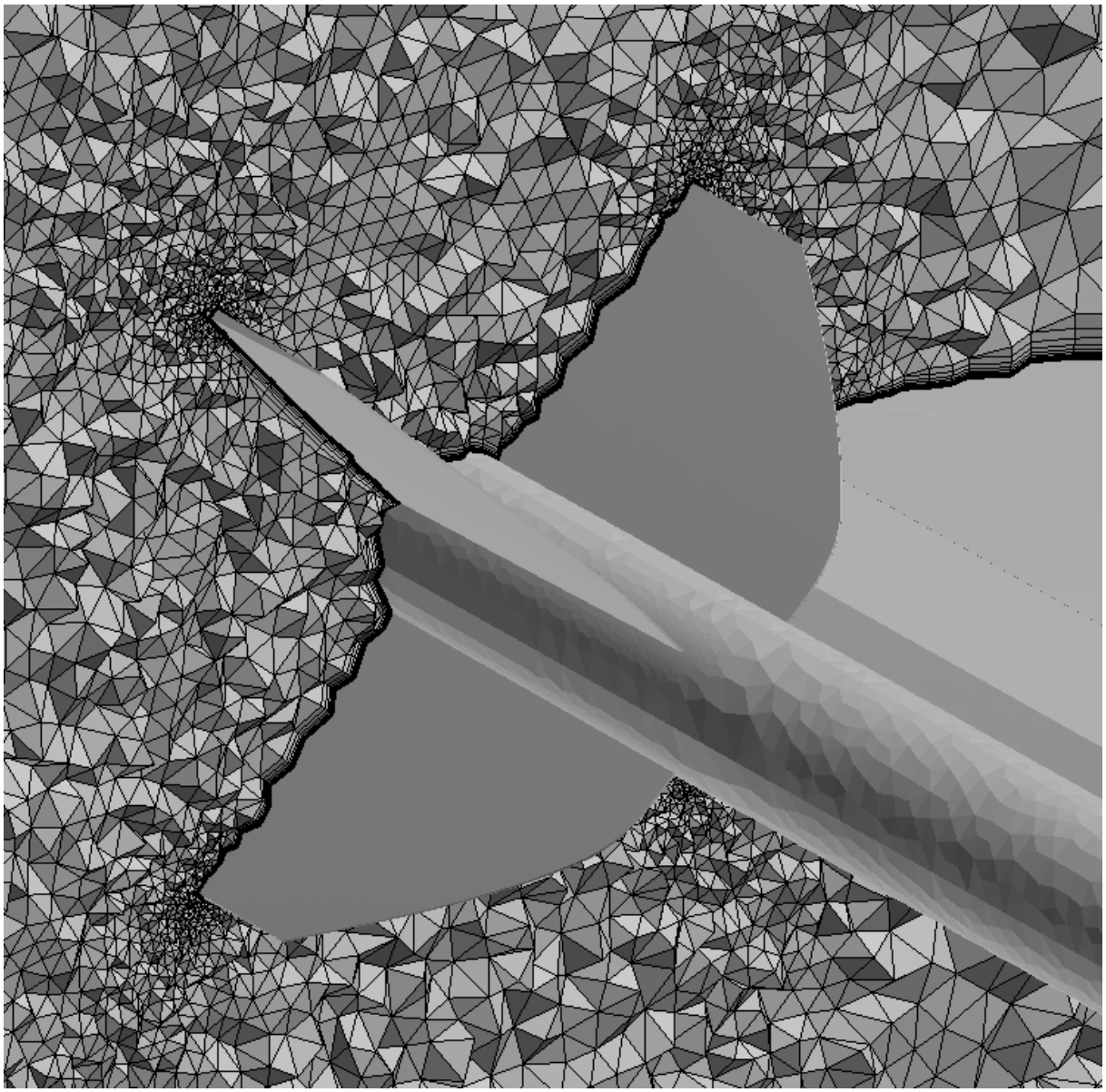

Figure 13-4: Crinkle Cut of Unstructured Mesh at Cut Through Tailfins of Wingtip Missile.

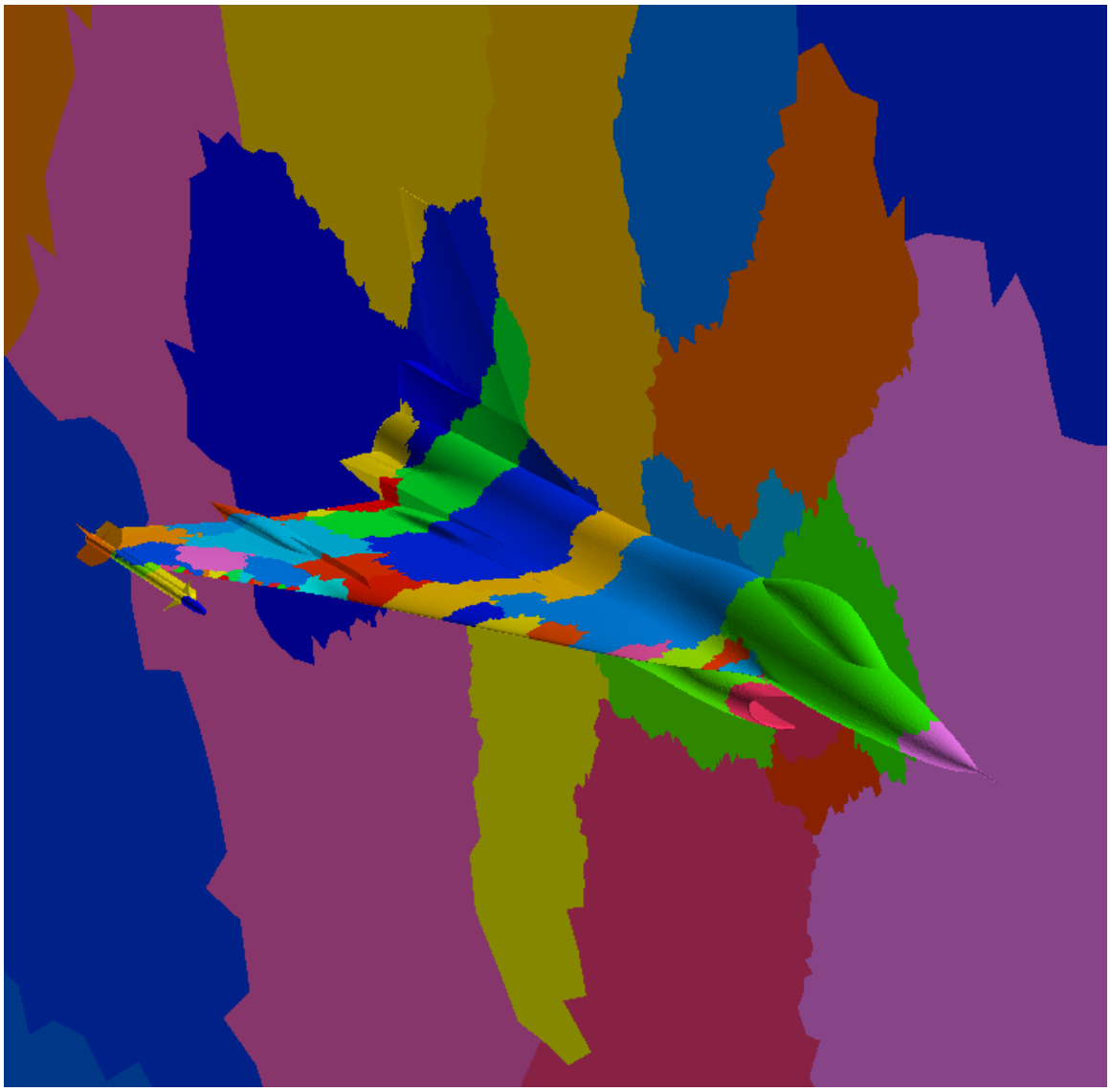

Figure 13-5: F-16XL Mesh was Partitioned to Run on 64 Processors.

13.5 RESULTS AND DISCUSSION

LM Aero produced CFD results for three of the seven cases shown in Table 13-1; FC7, FC19, and FC70. This gives two high-lift cases and one transonic case, yielding a representative cross-section of the relevant physics for this program. These cases are at zero nominal sideslip (although there is a small non-zero measured sideslip from the test), so all simulations are on half of the aircraft with symmetry conditions on the centerline plane. Although all of the sideslip angles are set to zero for symmetry, all other conditions are set to the exact value from the flight test.

13.5.1 Flight Condition 7

The first test case considered is FC7, which is one of the high-lift cases considered. The flight test data was taken at Mach number 0.304 at an altitude of 5000 feet, which gives a Reynolds number (based on mean aerodynamic chord) of 44.4 million. The angle of attack is 11.89 degrees. The pressure coefficient on the top surface of the wing is shown in Figure 13-6 for the full aircraft along with a detailed view of the outboard region of the wing. This clearly shows the strong suction peak on the leading edge near the wing root and outboard of the crank. The suction region follows the path of the vortices on the top surface and is evident on the inboard surface of the actuator pod. Figure 13-7 shows the path of the vortices using bounded cuts of total pressure. The primary vortex is clear, and the secondary vortex which forms next to the primary vortex is evident on close inspection. The vortex, which forms outboard of the crank, is also very clear. Also note the vortices being shed from the missile tailfins.

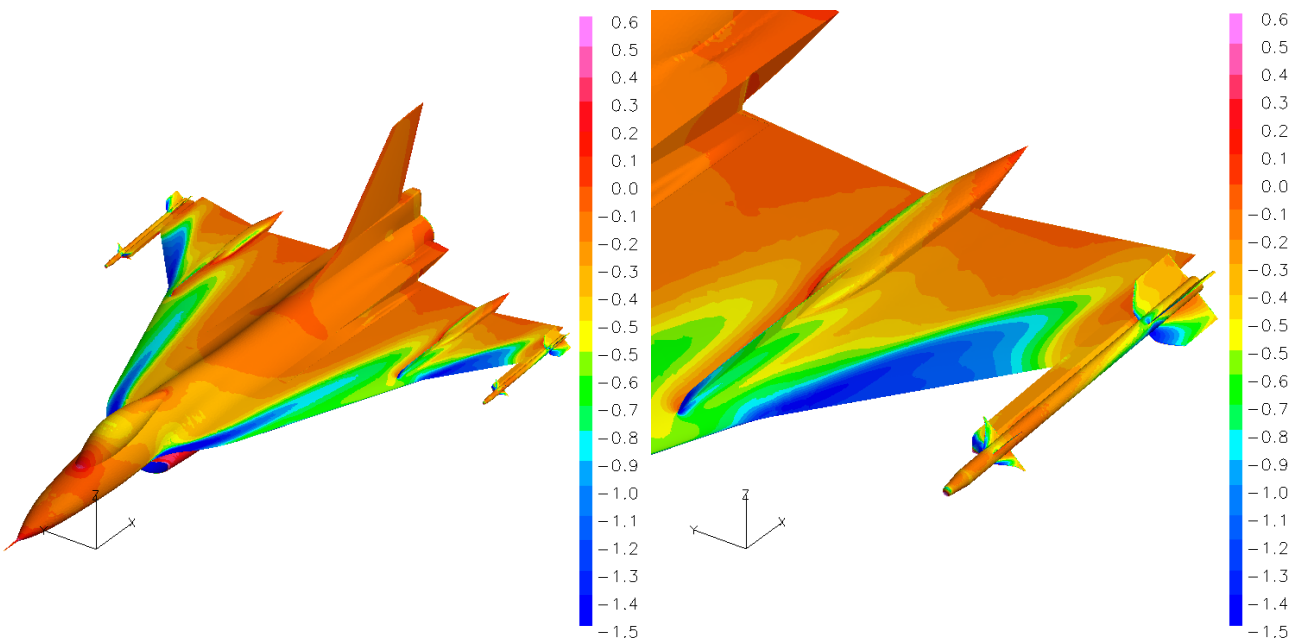

Figure 13-6: Surface C_p Distribution for FC7 on Upper Surface and Detail of Outboard Section of Wing.

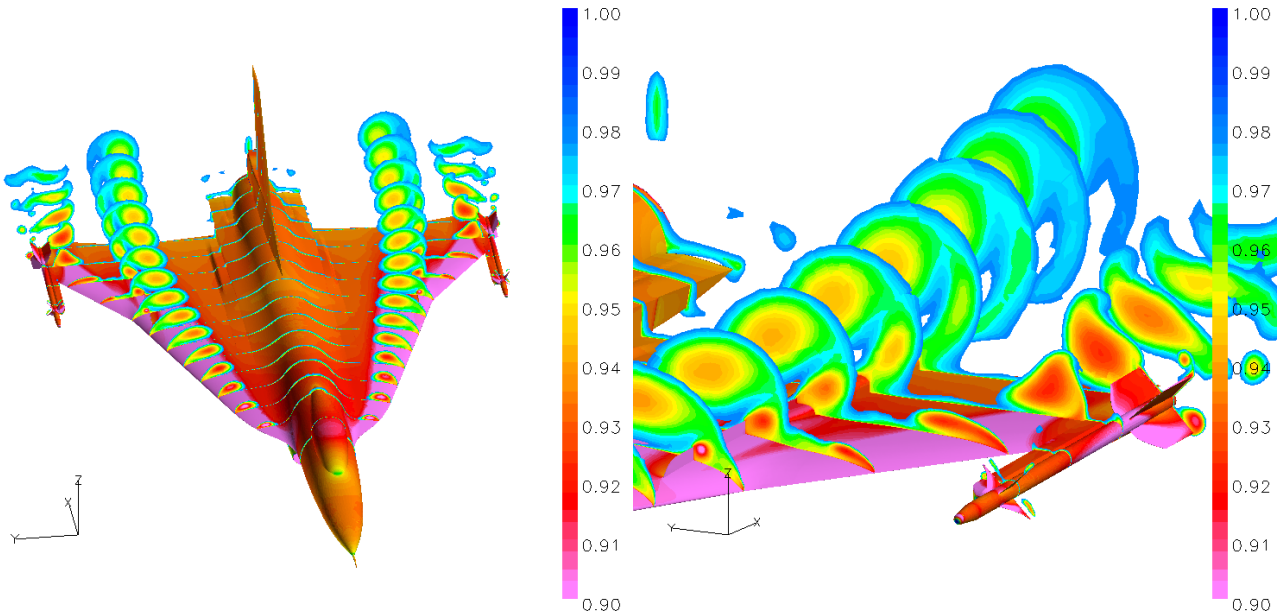

Figure 13-7: Bounded Total Pressure Cuts Colored by Total Pressure for FC7 Show Locations of Vortices.

The streamline pattern for this flow is shown with streamtubes colored by total pressure in Figure 13-8. The complexity of the flow pattern is evident from the streamlines. The primary vortex is plainly visible, as well as the secondary vortex, especially outboard of the air dam. The flow along the leading edge eventually wraps up into the third vortex outboard of the crank. Also evident is the total pressure loss in the center of the vortex cores.

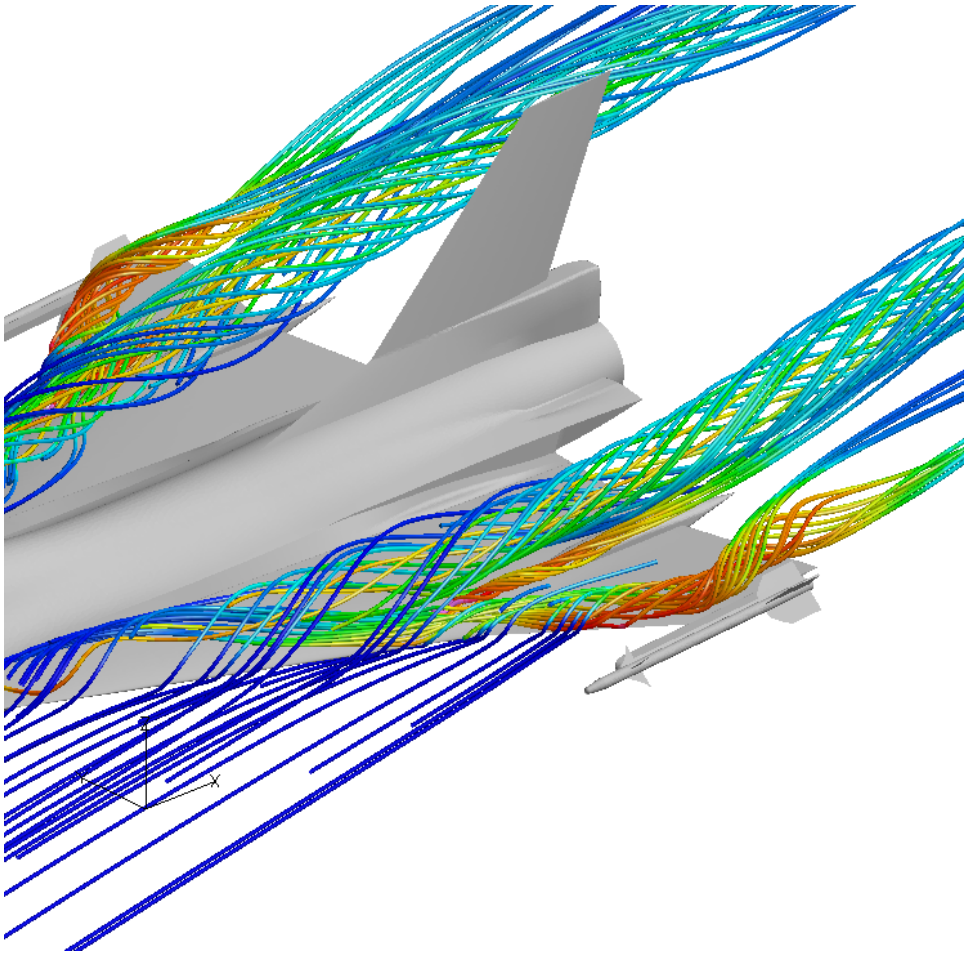

Figure 13-8: Streamtubes Colored by Total Pressure for FC7.

The pressure coefficient C_p was measured during the flight tests at specific buttlines (corresponding to the pressure belt placement) and fuselage stations. The CFD data was post-processed to compare to the C_p at these buttlines and fuselage stations. The buttline comparison for FC7 is shown in Figure 13-9. The CFD solver underpredicts the suction peak at each buttline except BL184.5, which does not have a suction peak. This may be the reason that the secondary vortex is not as evident as it should be. The C_p profile matches fairly well before and after the suction peak. This is important since the underprediction of the suction peak pressure does not seem to affect the solution elsewhere. The reason for the underprediction may be the flux limiter used. Previous experience with Falcon indicates that changing the parameters for the flux limiter may aid in prediction of the suction peak at high-lift conditions.

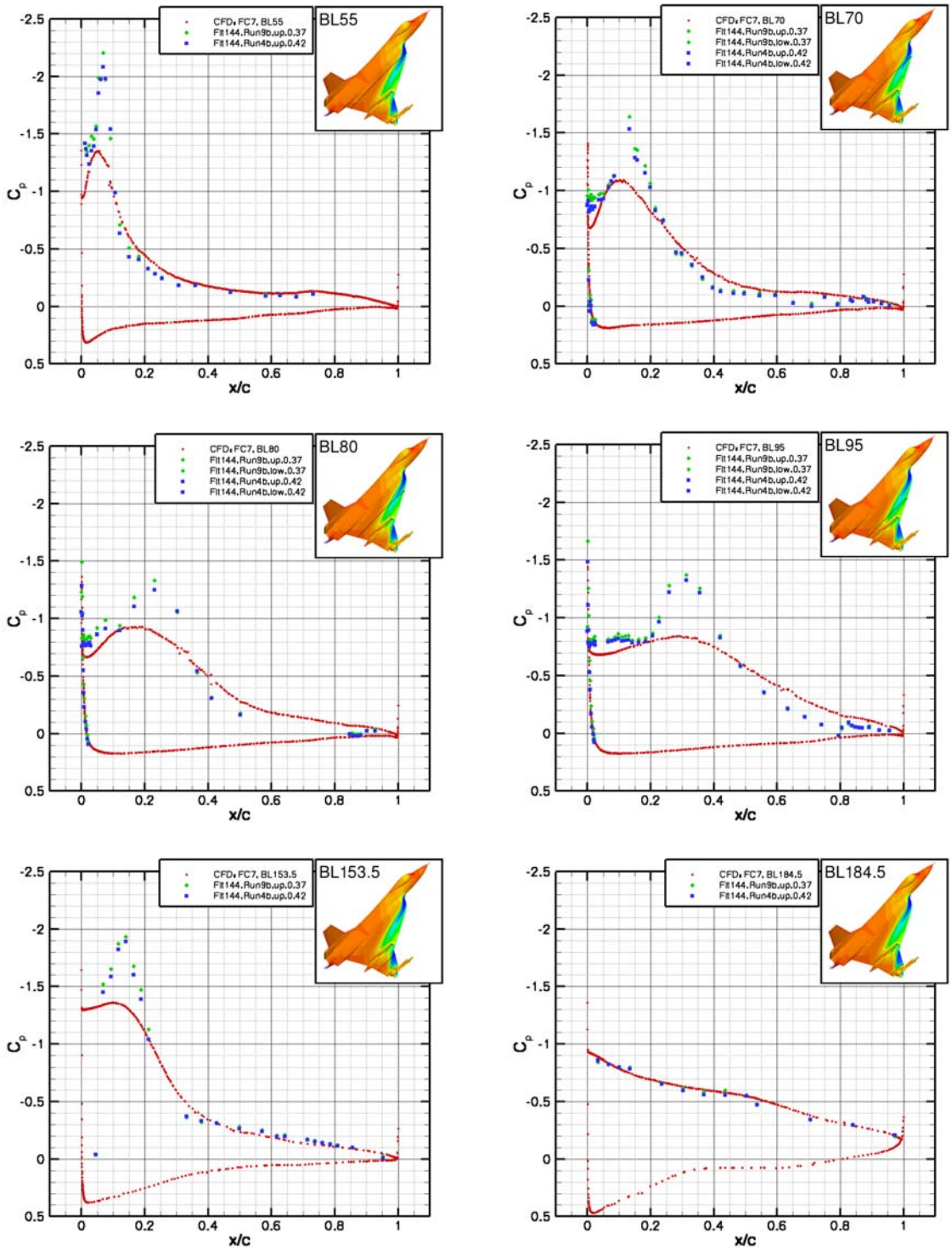

Figure 13-9: Comparison of C_p to Flight Test Data for FC7 at Various Buttlines.

The C_p distribution along the fuselage station cuts is shown in Figure 13-10. It is evident again at FS300 that the suction peak is underpredicted, but the rest of the comparisons are reasonable. At FS407.5 and FS450 the position of the air dam is evident by the discontinuous change in C_p at this location.

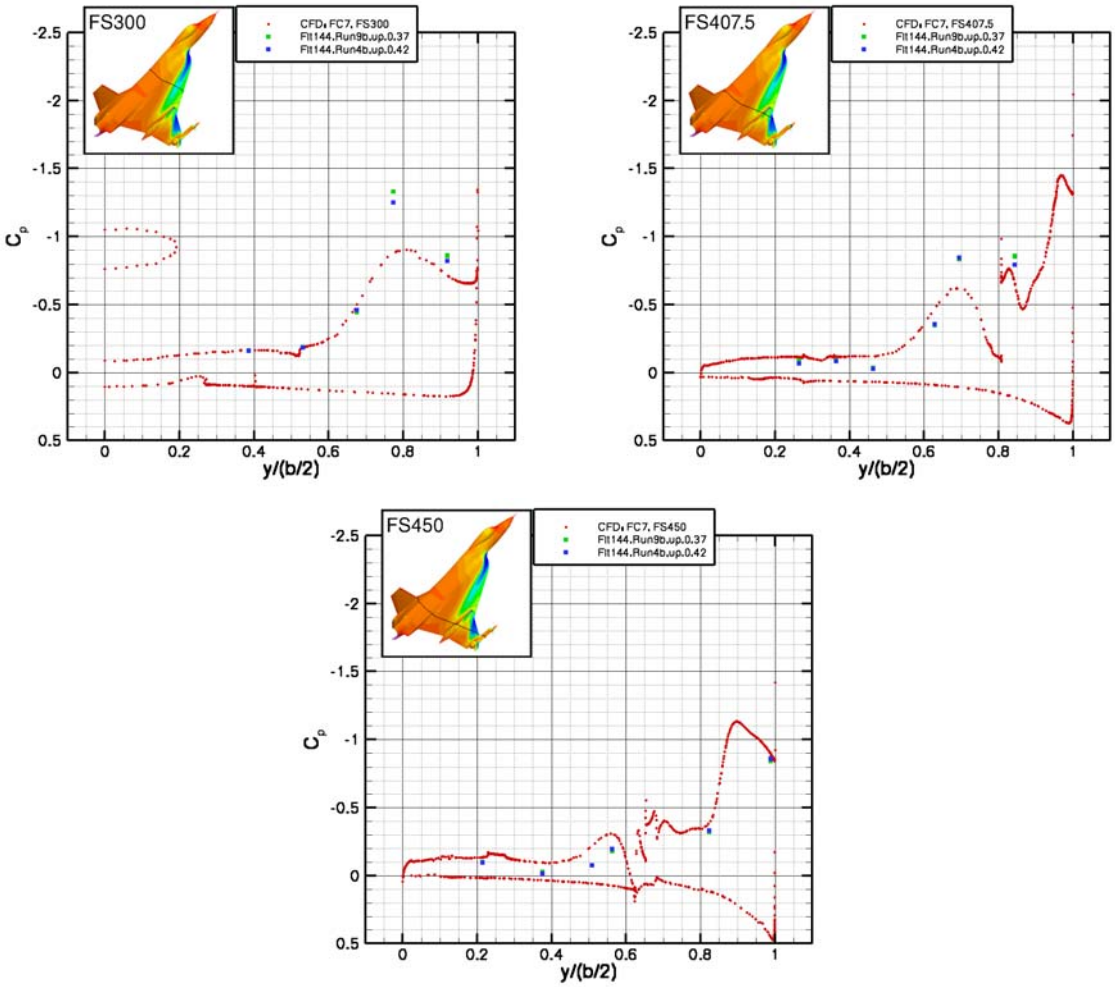

Figure 13-10: Pressure Comparison of C_p to Flight Test Data at Various Fuselage Stations for FC7.

The previous results show that the suction peak is missed consistently at each buttline and fuselage station location. A possible reason for this is excessive dissipation due to a low compression factor (1.0) in the flux limiter. Further simulations were performed at flight condition 7 using a compression factor of 1.4. The results at the same buttlines and fuselage stations are shown in Figure 13-11 and Figure 13-12 respectively. While increasing the compression factor does help increase the magnitude of the suction peak near the leading edge, it still does not raise it sufficiently to match the flight test data.

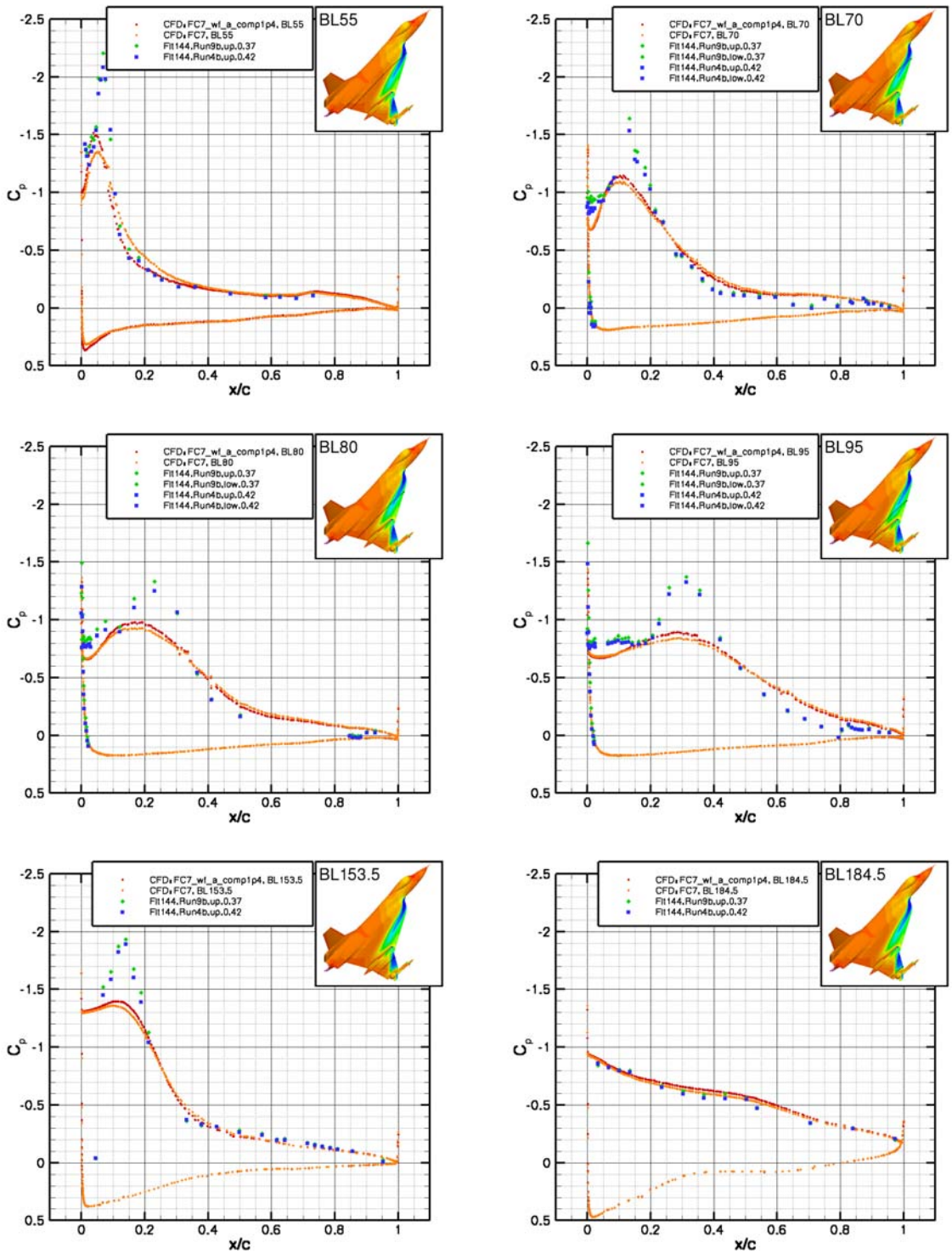

Figure 13-11: Pressure Coefficient Comparisons at Various Buttline Locations, Flux Limiter Compression Factors 1.0 and 1.4, FC7.

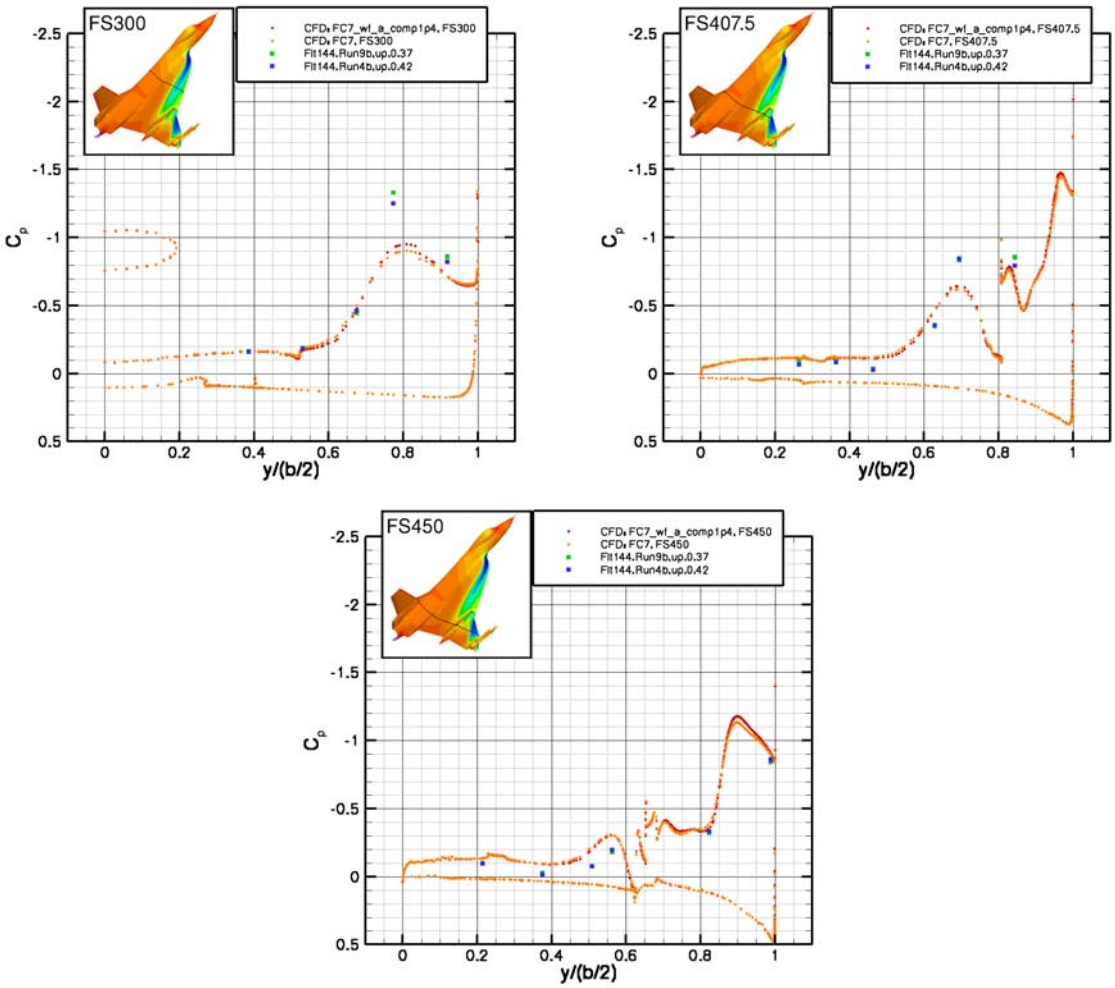

Figure 13-12: Pressure Coefficient Comparison at Various Fuselage Station Cuts, Flux Limiter Compression Factor of 1.0 and 1.4, FC7.

13.5.2 Flight Condition 19

The flight condition FC19 is very similar to FC7 with the exception of altitude (10000 feet). The Mach number is 0.36, the Reynolds number is 46.8 million, and the angle of attack is 11.85 degrees. The C_p surface plots (Figure 13-13) are almost identical for the two cases, with the only discernable difference in and around the engine inlet, which is due to a difference in inlet conditions. The total pressure surfaces seem to show differences (Figure 13-14), but this is due to the fact that the magnitude of the total pressure loss is higher for FC19. The shape and placement of the primary, secondary, and outboard vortices is the same for the two cases. The streamline pattern is almost identical as well (Figure 13-15), again with the only difference the total pressure coloring the streamtubes. All of the C_p plots, both buttline and fuselage station, are identical.

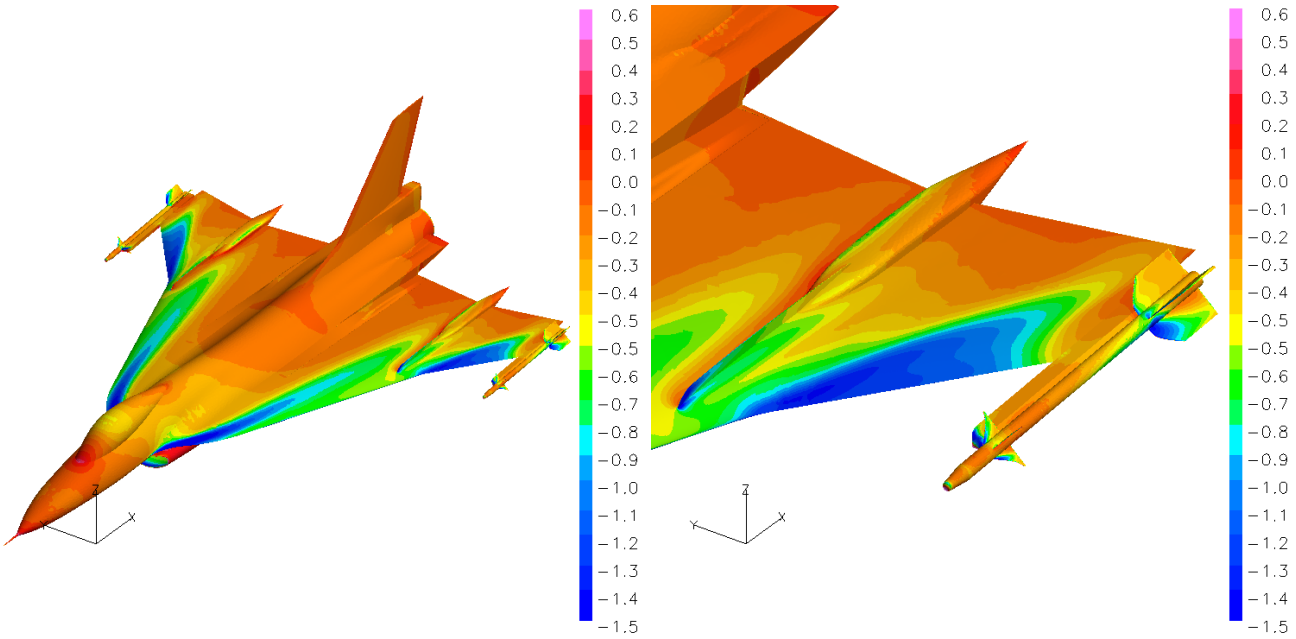

Figure 13-13: Surface C_p Distribution for FC19.

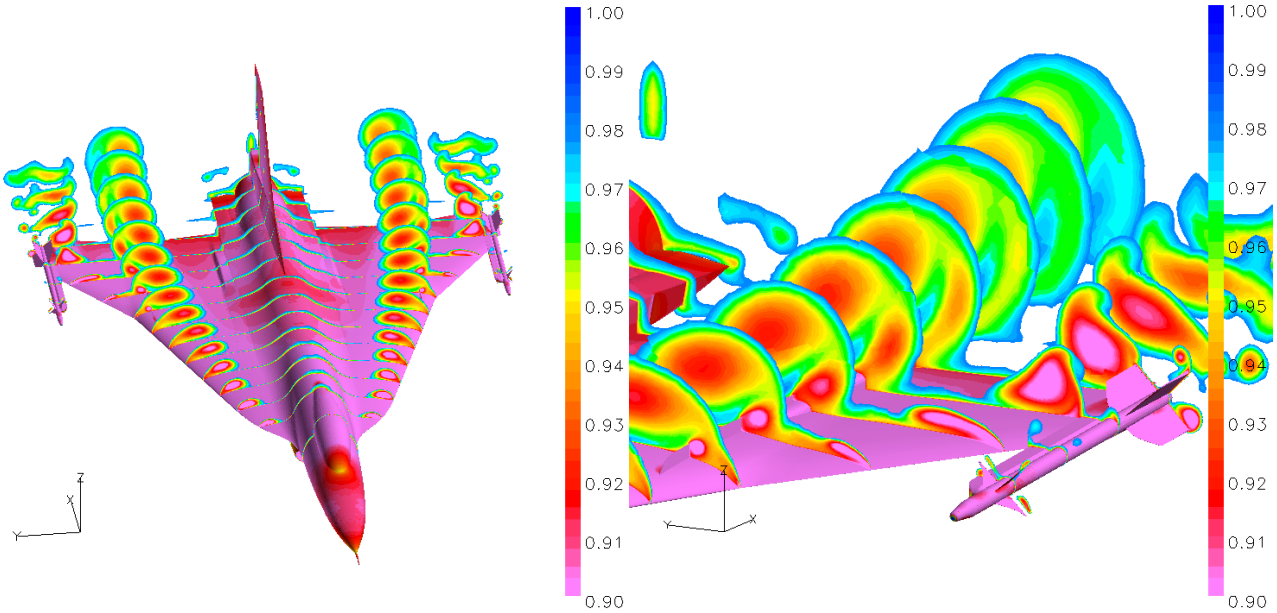

Figure 13-14: Bounded Total Pressure Cuts for FC19.

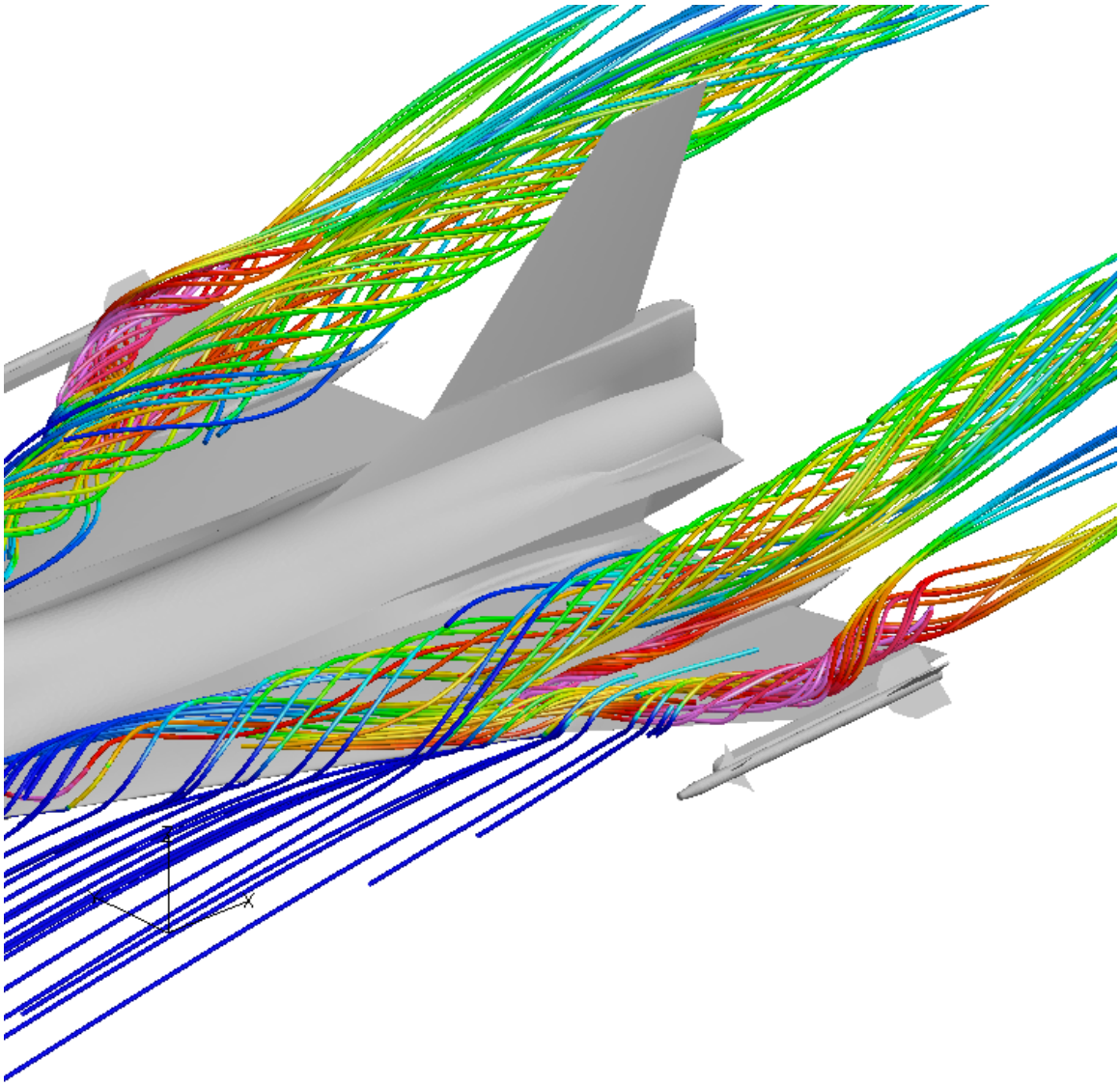

Figure 13-15: Streamtubes Colored by Total Pressure for FC19.

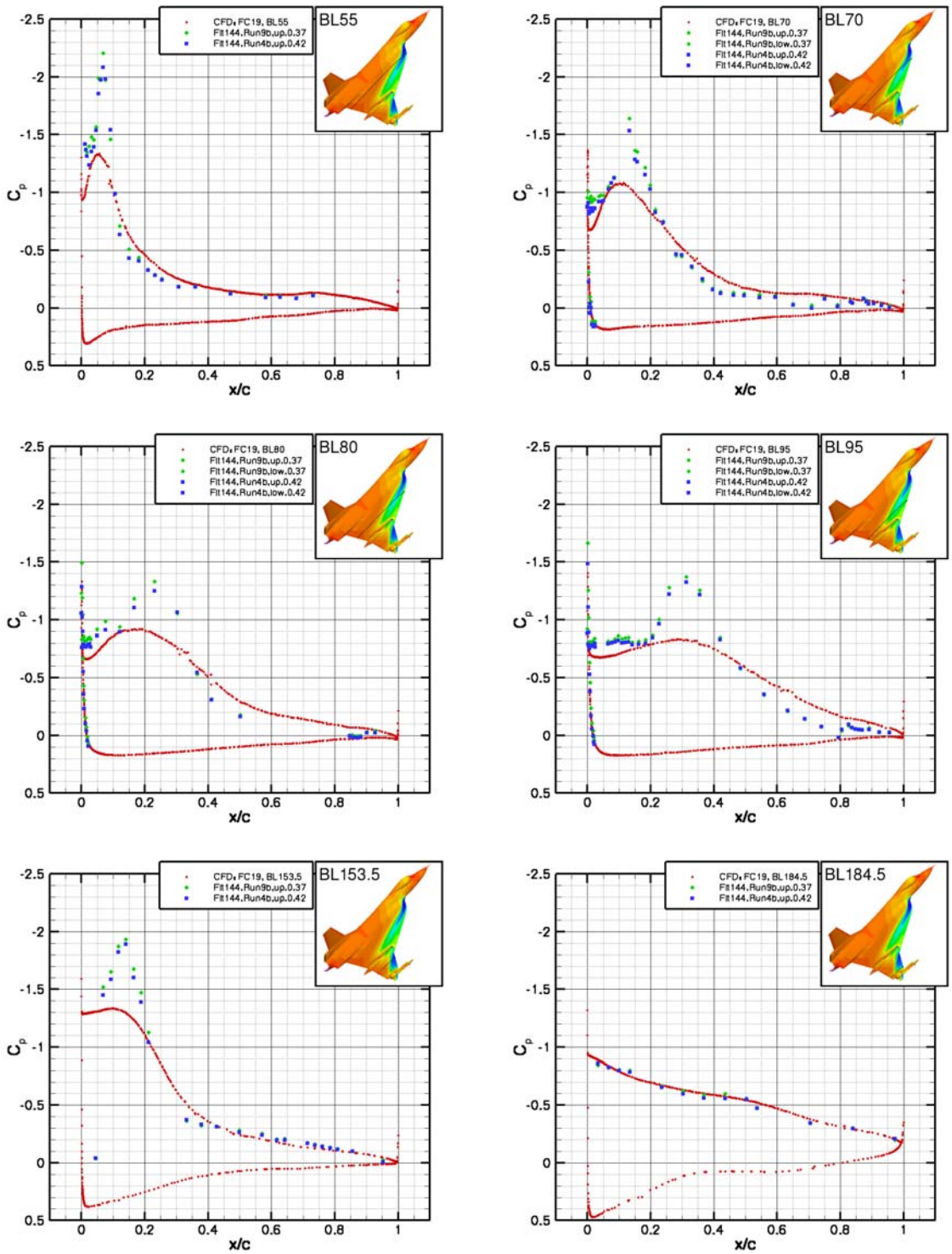

Figure 13-16: Comparison of C_p to Flight Test Data for FC19 at Various Buttlines.

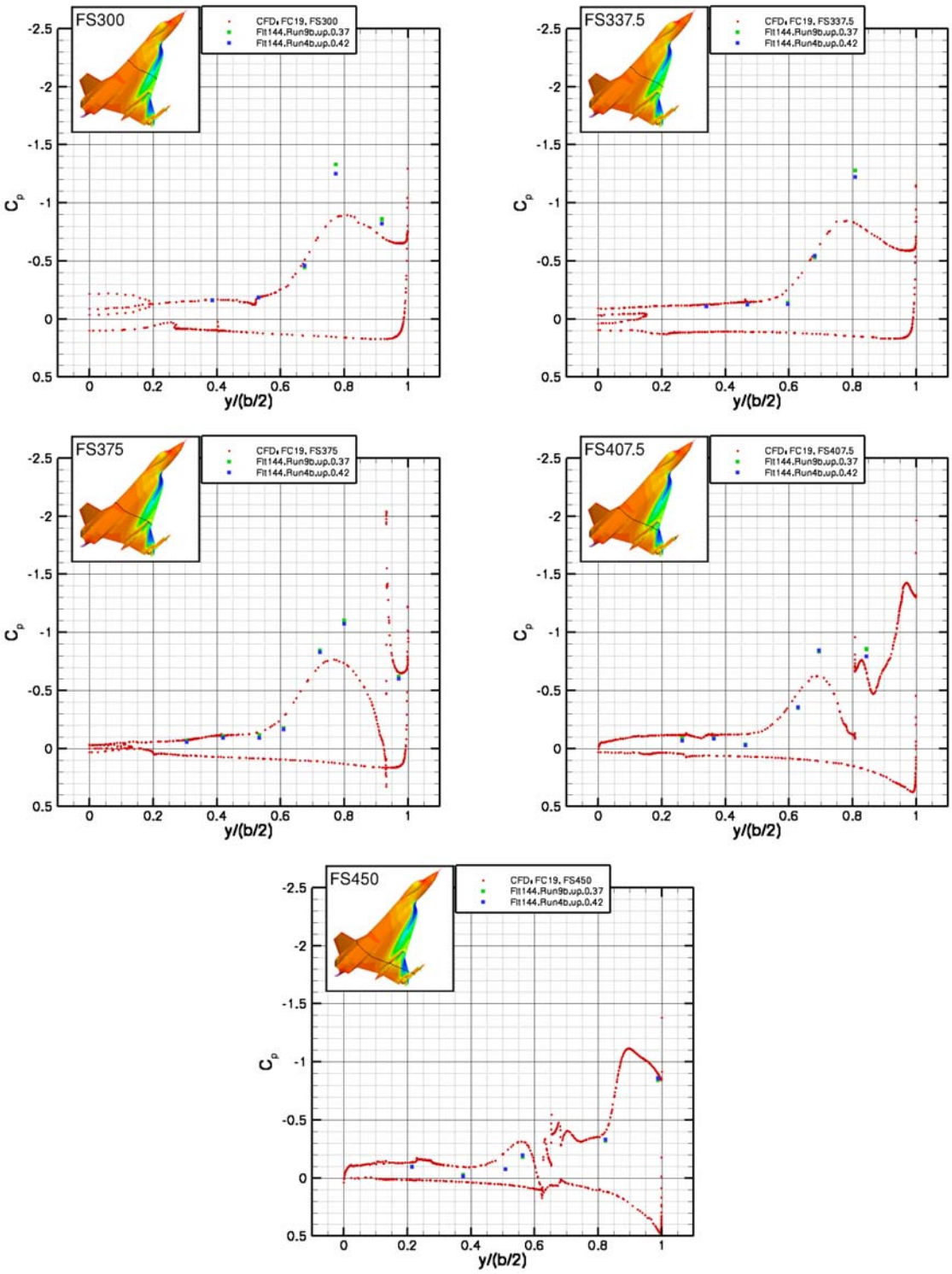

Figure 13-17: Comparison of C_p to Flight Test Data for FC19 at Various Fuselage Stations.

13.5.3 Flight Condition 70

The only transonic case is FC70, which has a Mach number of 0.97. The angle of attack is low relative to the rest of the test suite (4.4 degrees), and hence the vortex structure is much less pronounced at this case. The flight test data was taken at an altitude of 22,300 feet, which yields a Reynolds number of 88.77 million. The shock structure is the dominant mechanism at these flight conditions. Iso-surfaces at Mach 1 are shown in Figure 13-19 (colored by total pressure), and these clarify the C_p surface plots shown in Figure 13-18. There are three large Mach surfaces which terminate in very weak shocks. The first starts and terminates on the canopy, the second starts very near the inboard leading edge and terminates at the middle of the inboard wing section, and the third starts roughly at the crank and terminates at the trailing edge. There is a region of smaller Mach surfaces that sit between the second and third large surfaces, which also seem to terminate in very weak shocks. Looking at the surface C_p distribution, the shock locations are evident from the pressure rise. Note also the Mach 1 surfaces at the missile nose, shoulder, and forward fins.

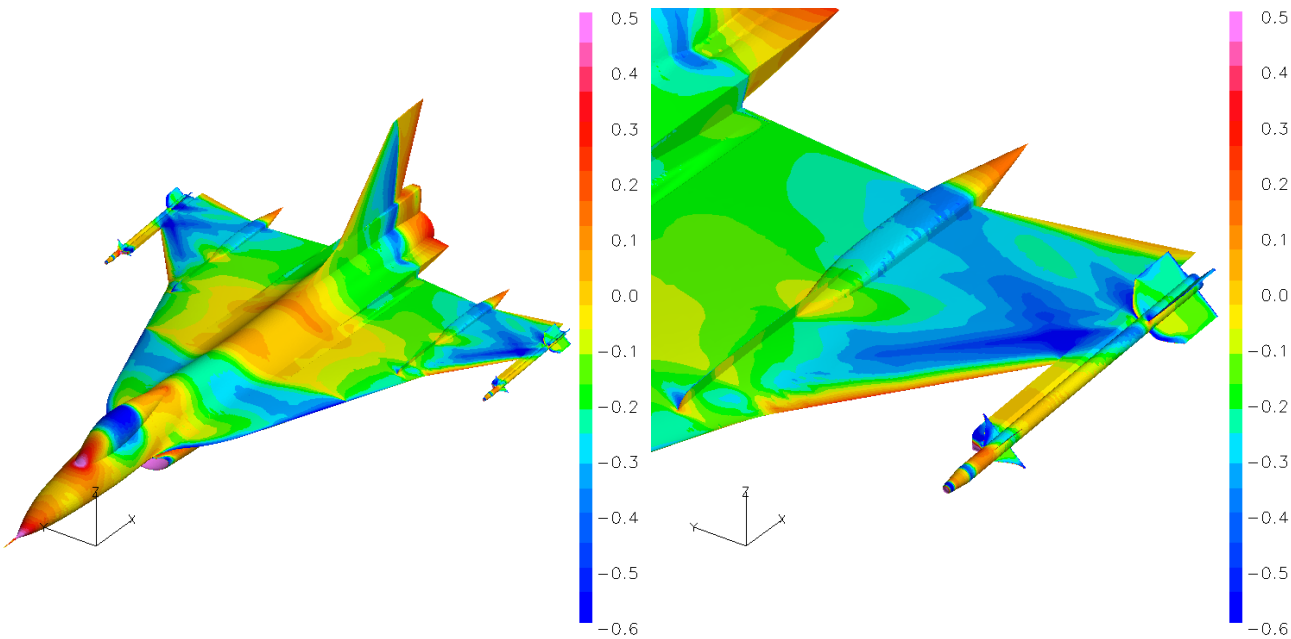

Figure 13-18: Surface C_p Distribution for FC70.

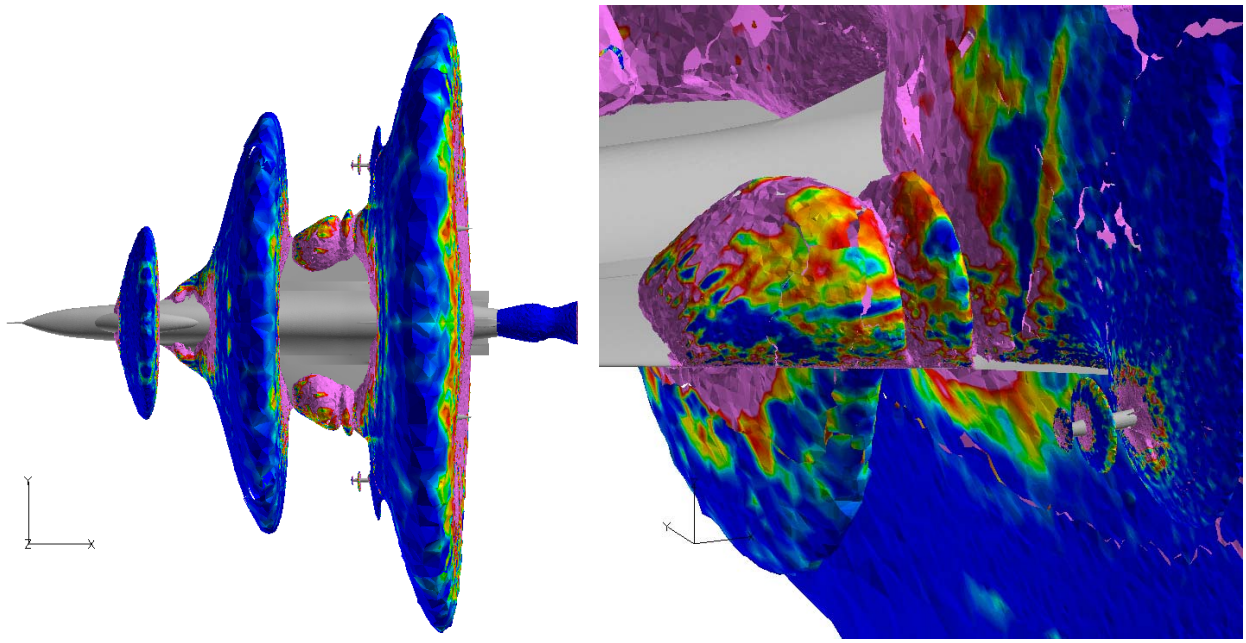

Figure 13-19: Mach 1.0 Iso-Surfaces Colored by Total Pressure for FC70.

The buttline C_p matches reasonably well with the flight test (Figure 13-20) at BL55 and BL95, but does not match very well at other buttlines. This disparity is also evident in the fuselage stations comparisons, with the exception of FS407.5. The reason for the gross differences at this flight condition are unknown at the present time, but the consistency of the differences across a range of different flow solvers and grids suggests that there is a difference between the configuration and flow conditions in the test and those simulated in the CFD.

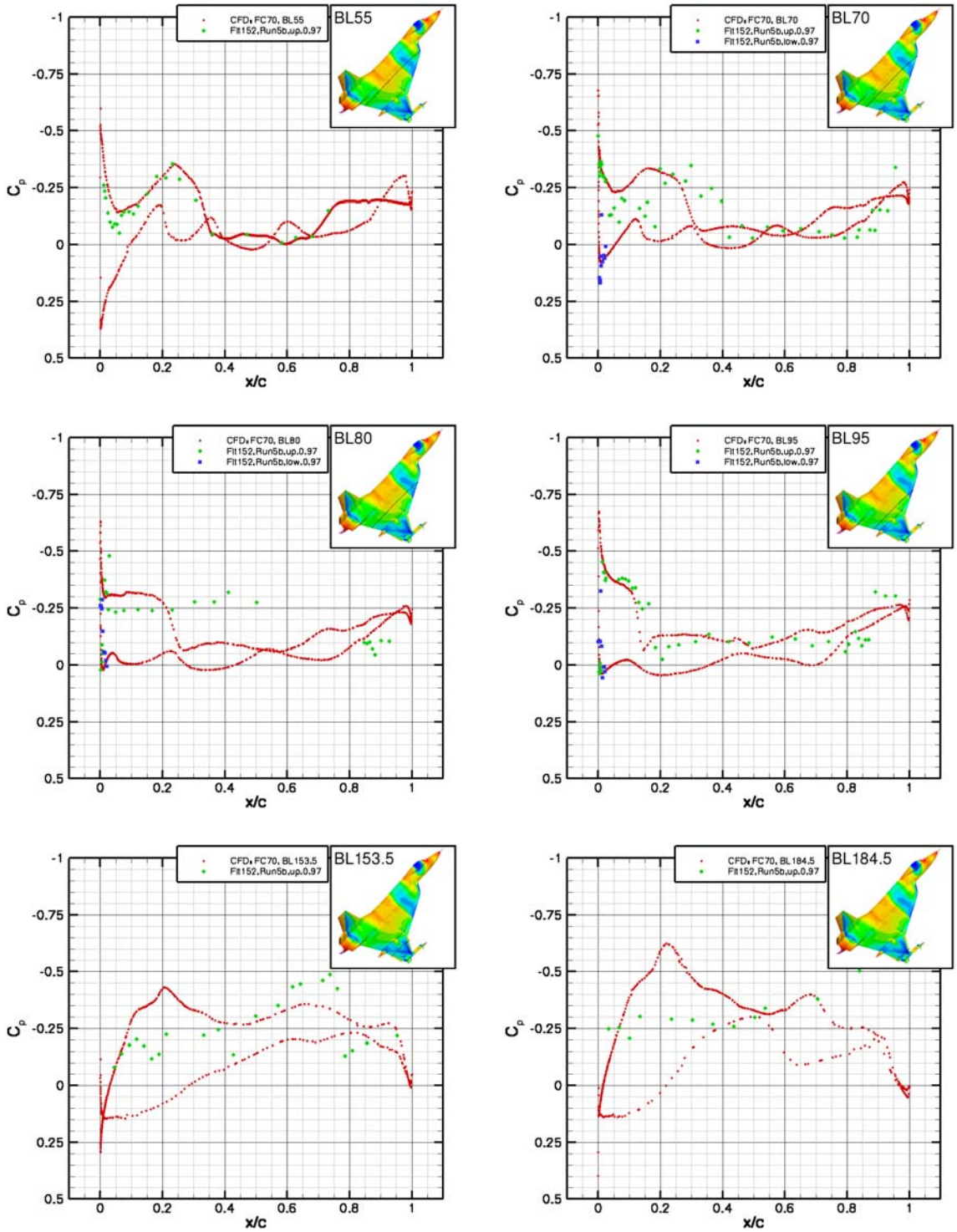

Figure 13-20: Comparison of C_p to Flight Test Data for FC70 at Various Buttlines.

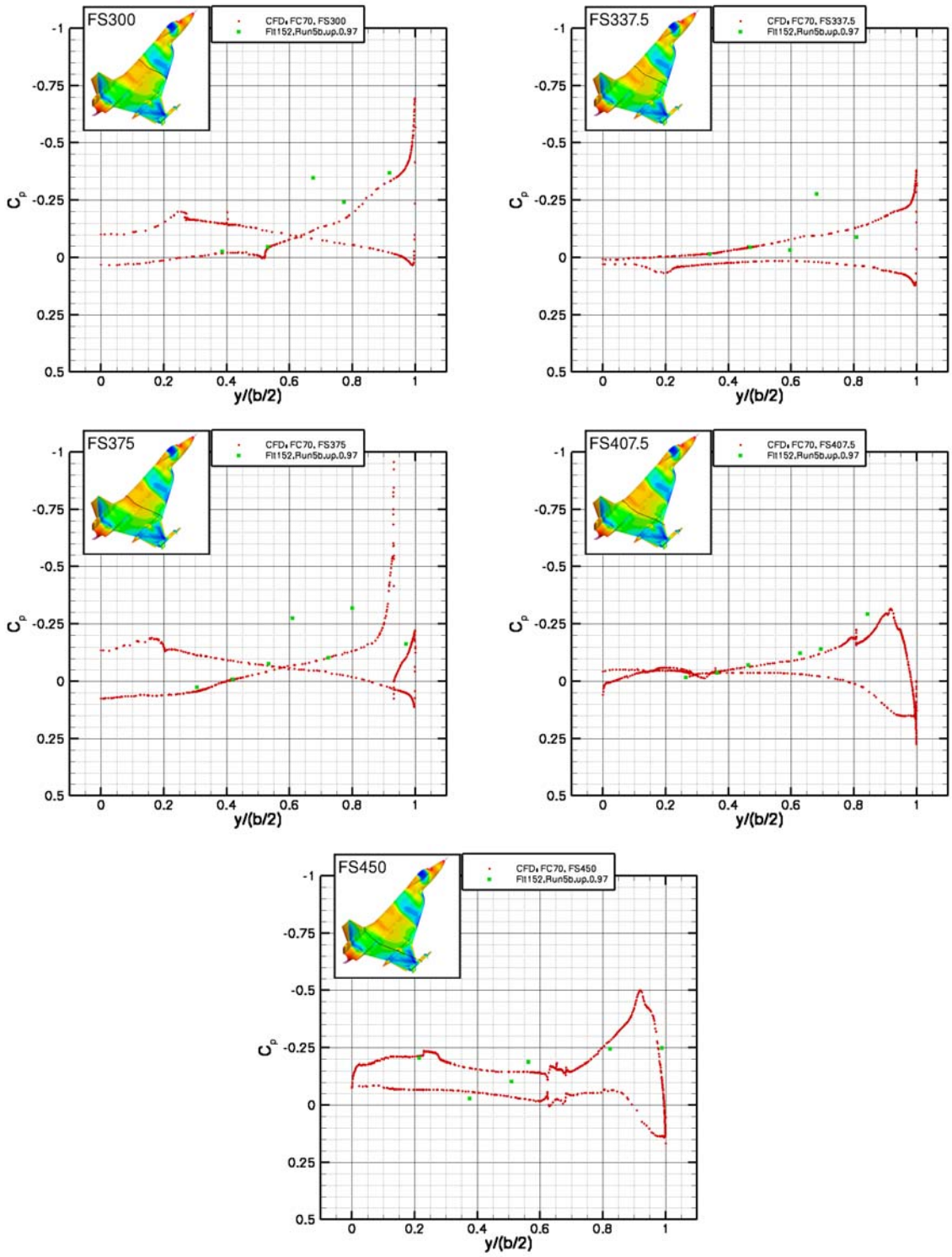

Figure 13-21: Comparison of C_p to Flight Test Data for FC70 at Various Fuselage Stations.

13.6 CONCLUSIONS

The LM Aero general purpose flow solver Falcon v4 was used to run simulations on the F-16XL geometry at high-lift and transonic flight conditions for which flight test data exists as part of the CAWAPI program. The hybrid computational mesh was produced by the UT SimCenter. The results were generally encouraging, with Falcon capturing the major flow features and placement. The suction peak at the leading edge of the wing was underpredicted, however, for all high-lift cases. This is partially due to the compression factor setting for the flux limiter. This does not totally account for the differences in the suction peak values, as an experiment raising the compression factor showed. The most likely reason for the discrepancy is that the simulations cited here used wall functions with a correspondingly coarser grid in the near wall region than one would use for a full viscous simulation. The use of wall functions seems to be inadequate for these types of problems. The C_p comparison to flight test at the transonic condition was poor at almost all buttlines and fuselage stations. There is good agreement, though, with the simulations performed by other flow solvers. The best explanation for this is that the geometric configuration or flow conditions simulated in the CFD are different from those used in the flight test.

13.7 REFERENCES

[13-1] Lamar, J.E., Obara, C.J., Fisher, B.D. and Fisher, D.F.: *Flight, Wind-Tunnel, and Computational Fluid Dynamics Comparison for Cranked Arrow Wing (F-16XL-1) at Subsonic and Transonic Speeds*, NASA/ TP-2001-210629, February 2001.

[13-2] Lamar, J.E. and Obara, C.J.: *Review of Cranked-Arrow Wing Aerodynamics Project: Its International Aeronautical Community Role*, AIAA Paper 2007-0487, Presented at 45th AIAA Aerospace Sciences Meeting and Exhibit, Reno, NV, January 2007.

[13-3] Roe, P.L.: *Characteristic-Based Schemes for the Euler Equations*, Annual Review of Fluid Mechanics, Vol. 18, 1986, pp. 337-365.

[13-4] Smith, B.R.: *The k-kl Turbulence Model and Wall Layer Model for Compressible Flows*, AIAA Paper 90-1483, June 1990.

[13-5] Reed, C.L., Karman, S.L. and Anderson, D.A.: *Implementation of Low Speed Preconditioning in the Splitflow Code*, AIAA Paper 97-1867, June 1997.

[13-6] Karypis, G. and Kumar, V.: *A Fast and High Quality Multilevel Scheme for Partitioning Irregular Graphs*, SIAM Journal on Scientific Computing, Vol. 20, No. 1, pp. 359-392, 1999.

[13-7] Karman, S., Mitchell, B. and Sawyer, S.: *Unstructured Grid Solutions of CAWAPI F-16XL by UT SimCenter*, AIAA Paper 2007-0681, Presented at 45th AIAA Aerospace Sciences Meeting and Exhibit, Reno, NV, January 2007.

[13-8] Karman, S.L. Jr.: *Unstructured Viscous Layer Insertion Using Linear-Elastic Smoothing*, AIAA-2006-0531, January 2006.